trometer is operated by the Brisbane NMR Centre.

References and Notes

(1) Alfrey, T.; Lavin, E. *J. Am. Chem. Soc.* **1945**, *67*, 2044.
(2) Bamford, C. H.; Barb, W. G. *Discuss. Faraday Soc.* **1953**, 208.
(3) Huglin, M. B. *Polymer* **1962**, *3*, 335.
(4) Tsuchida, E.; Ohtani, Y.; Nakadai, H.; Shinohara, I. *Kogyo Kagaku Zasshi* **1967**, *70*, 573.
(5) Roth, H.; Arnold, M.; Raetzsch, M. *Acta Polym.* **1981**, *32*, 277.
(6) Barb, W. G. *J. Polym. Sci.* **1953**, *11*, 117.
(7) Enomoto, G.; Ogo, Y.; Imoto, T. *Macromol. Chem.* **1970**, *138*, 19.
(8) Tsuchida, E.; Tomono, T.; Sano, H. *Makromol. Chem.* **1972**, *151*, 245.
(9) Raetzsch, M.; Arnold, M.; Hoyer, R. *Plaste Kautsch.* **1977**, *24*, 731.
(10) Dodgson, K.; Ebdon, J. R. *Eur. Polym. J.* **1977**, *13*, 791.
(11) Capek, I.; Barton, J. *Macromol. Chem.* **1981**, *182*, 3505.
(12) Arnold, M.; Raetzsch, M. *Plaste Kautsch.* **1982**, *29*, 381.
(13) Braun, D.; Czerwinski, W. *Makromol. Chem.* **1983**, *184*, 1071.
(14) Tsuchida, E.; Tomono, T. *Makromol. Chem.* **1971**, *141*, 265.
(15) Yoshimura, M.; Nogami, T.; Yokayama, M.; Mikawa, H.; Shirota, Y. *Macromolecules* **1976**, *9*, 211.
(16) Arnold, M.; Raetzsch, M.; Osterode, J. *Acta Polym.* **1983**, *34*, 272.
(17) Rzaev, Z. M.; Bryksina, L. V.; Sadykh-zade, S. I. *J. Polym. Sci., Polym. Symp.* **1973**, *No. 42*, 519.
(18) Iwatsuki, S.; Itoh, T.; Hiraiwa, A. *Makromol. Chem.* **1981**, *182*, 2161.
(19) Dodgson, K.; Ebdon, J. R. *Makromol. Chem.* **1979**, *180*, 1251.
(20) Farmer, R. G.; Hill, D. J. T.; O'Donnell, J. H. *J. Macromol. Sci., Chem.* **1980**, *A14*, 51.
(21) Cais, R. E.; Farmer, R. G.; Hill, D. J. T.; O'Donnell, J. H. *Macromolecules* **1979**, *12*, 835.
(22) Hill, D. J. T.; O'Donnell, J. H.; O'Sullivan, P. W. *Macromolecules* **1983**, *16*, 1295.
(23) Buchak, B. E.; Ramey, K. C. *J. Polym. Sci., Polym. Lett. Ed.* **1976**, *14*, 401.
(24) Barron, P. F.; Hill, D. J. T.; O'Donnell, J. H.; O'Sullivan, P. W. *Macromolecules*, in press.
(25) Tidwell, P. W.; Mortimer, G. A. *J. Polym. Sci., Part A* **1965**, *3*, 369.
(26) Tidwell, P. W.; Mortimer, G. A. *J. Macromol. Sci., Rev. Macromol. Chem.* **1970**, *C4*, 281.
(27) Behnken, D. W. *J. Polym. Sci., Part A* **1964** *2*, 645.
(28) McFarlane, R. C.; Reilly, P. M.; O'Driscoll, K. F. *J. Polym. Sci., Polym. Chem. Ed.* **1980**, *18*, 251.
(29) Leicht, R.; Fuhrmann, J. *J. Polym. Sci., Polym. Chem. Ed.* **1983**, *21*, 2215.
(30) Yamada, B.; Itahashi, M.; Otsu, T. *J. Polym. Sci., Polym. Chem. Ed.* **1978**, *16*, 1719.
(31) Natansohn, A.; Galea, D.; Percec, V.; Simionescu, C. I. *J. Macromol. Sci., Chem.* **1981**, *A15*, 393.
(32) According to the formula

$$\frac{SS(\hat{\theta})_B - SS(\hat{\theta})_A}{p_A - p_B} \Big/ \frac{SS(\hat{\theta})_A}{n - p_A} \geq F_{\alpha(p_A - p_B, n - p_A)}$$

where model B is a special case of model A. Model A provides a significant improvement over model B if the inequality is true.
(33) Beale, E. M. L. *J. R. Stat. Soc.* **1960**, 41.
(34) Hill, D. J. T.; O'Donnell, J. H.; O'Sullivan, P. W., unpublished data.
(35) Green, J. R.; Margerison, D. "Statistical Treatment of Experimental Data", 2nd ed.; Elsevier: Amsterdam, 1978; Chapter 8.
(36) Olson, K. E.; Butler, G. B. *Macromolecules* **1983**, *16*, 707.

Free-Radical Copolymerization. 3. Determination of Rate Constants of Propagation and Termination for the Styrene/Methyl Methacrylate System. A Critical Test of Terminal-Model Kinetics[1]

Takeshi Fukuda,* Yung-Dae Ma, and Hiroshi Inagaki

Institute for Chemical Research, Kyoto University, Uji, Kyoto 611, Japan.

Received April 23, 1984

ABSTRACT: The validity of terminal-model kinetics of free-radical copolymerization was critically tested against a complete set of experiments carefully carried out on the bulk copolymerization of styrene and methyl methacrylate at 40 °C. The experiments involved determining the copolymer composition, the initiation rate, the polymerization rate, the volume contraction factor, and the radical lifetime, and thus the rate constants of propagation and termination were individually evaluated as a function of monomer composition. In the rotating-sector experiments, a new system was introduced which automatically measures the migration rate of the dilatometer meniscus with high precision. The following results were obtained: The copolymer composition conforms to the terminal model (Mayo–Lewis equation) within experimental error, whereas the propagation rate constant is entirely different from what the model predicts. As far as numerical values are concerned, the experimental data are well represented by the penultimate model. As to the termination step, the previous results indicating large, composition-dependent values of the Walling cross-termination factor ϕ are erroneous, since the validity of the terminal model is assumed in those analyses. The observed values of the termination rate constant are well represented by the chemical model with $\phi = 1$ as well as by the North diffusion model.

Introduction

The composition curves of most free-radical copolymerizations are, at least to good approximations, represented by the terminal-model equation, commonly termed the Mayo–Lewis equation.[2] This is equivalent to saying that the ratios of the propagation rate constants (reactivity ratios) are effectively constant, independent of feed-monomer composition. It seems that this is one of the main reasons why no serious doubt has ever been thrown on the essential validity of terminal-model kinetics.

Recently, we[3] noted that the composition curve for a *p*-chlorostyrene–methyl acrylate system exhibits significant deviations from the terminal-model curve, which could be interpreted, at least numerically, by the penultimate model.[4] Hill et al.,[5] who studied the composition and the sequential distributions of a styrene–acrylonitrile system,

0024-9297/85/2218-0017$01.50/0

showed that their system is better represented by the penultimate model rather than by the terminal and other models. It is believed that these findings would hardly have been obtained without the unusually elaborate studies carried out by these workers, and this stresses importance of such studies. Of the great number of reactivity ratio values reported in the literature, relatively few seem to have been established with adequate justification of the assumed terminal model. Accordingly, one should not hasten to conclude that the failure of the Mayo–Lewis equation is particularly exceptional.

It is more important to note that even if the constancy of the ratios is fully established, it does not necessarily imply constancy of the individual rate constants. Nevertheless, the terminal model has never been tested in this respect, except for a few limited cases.[6,7] In almost all the previous studies dealing with rate equations of copolymerization, the propagation step was assumed to obey the terminal model, and the central question was concerned with the mechanism of the termination step. Among the several rate equations so far proposed along this line,[6,8-14] that of Walling[8] has the simplest structure, permitting evaluation of the cross-termination factor ϕ (see eq 22) from the data on the rates of polymerization and initiation only, and has been applied to a wide variety of systems. To summarize the results, most systems exhibit values of ϕ which are much larger than one and, in many cases, dependent on feed-monomer composition.[8,14-37] Systems which have a ϕ value close to 1 are rather exceptional.[6,32,38,39] This is in sharp contrast to the reactions between low molecular weight radicals, which are characterized by ϕ virtually equal to 1 in almost all cases.[24,40,41] The origin of this "unusual" behavior of copolymerization systems is as yet understood very little.

We have doubted the general validity of terminal-model kinetics and for some years have been collecting basic experimental data to make a stringent test of the model.[1,3,37,42] In this paper, we report results of such a test which was made on the bulk-copolymerization of styrene (ST, monomer 1) and methyl methacrylate (MMA, monomer 2) at 40 °C. This system is known to be well represented by the terminal model with respect to the composition and characterized by relatively large, composition-dependent values of ϕ.[8,15-19] In these respects, this is a "typical" copolymerization system. In order to obtain internally consistent results, we have measured all the parameters that are necessary to evaluate the rate constants of propagation and termination individually as a function of monomer composition. Those parameters include the copolymer composition, the rate of steady-state polymerization, the rate of initiation, the volume contraction factor, and the radical lifetime. In each experiment, we have carried out as many independent runs as possible, which should be effective to decrease experimental errors of random nature. To our knowledge, this is the first report that presents a complete set of kinetic data on a copolymerization system.

Theoretical Section

General Aspects of Copolymerization. To make clear the basic assumptions involved and the physical significance of the experimental information obtained in this study, we first consider some general aspects of the copolymerization of two monomers with or without added solvent(s).

We assume that the rates of initiation, R_i, propagation, R_p, and termination, R_t, are represented by eq 1–3, respectively, and that other reactions have no significant influence on the rate equations.

$$R_i = 2f'k_d[I] \tag{1}$$

$$R_p = \sum_i^r \sum_j^m k_{ij}[P_i\cdot][M_j] \tag{2}$$

$$R_t = \sum_i^r \sum_j^r k_{tij}[P_i\cdot][P_j\cdot] \tag{3}$$

In eq 1, [I] is the concentration of the initiator with a decomposition rate constant k_d and efficiency f'. Both k_d and f', and hence the factor $2f'k_d$ are a function of the feed composition. In eq 2 and 3, k_{ij} is the rate constant for the (polymeric) radical i to add monomer j, k_{tij} is the rate constant of termination between the radicals i and j, and $[P_i\cdot]$ and $[M_j]$ are the concentrations of the specified radical and monomer, respectively. The number r of *kinetically distinguishable* radicals over which the summations in eq 2 and 3 extend depends on the models considered for the propagation and termination reactions: for example, r is 2 for the terminal model and 4 for the penultimate model. Similarly, the number m of kinetically distinguishable monomers is not necessarily 2: if, for example, the monomer–monomer or solvent–monomer complex formation is important, it may be different from 2.

We define the (average) rate constants of propagation, k_p, and termination, k_t, by

$$R_p = k_p[P\cdot][M] \tag{4}$$

$$R_t = k_t[P\cdot]^2 \tag{5}$$

where $[P\cdot]$ and [M] are the total concentrations of the radicals and monomers:

$$[P\cdot] = \sum_i^r [P_i\cdot] \tag{6}$$

$$[M] = \sum_j^m [M_j] \tag{7}$$

Comparison of eq 2 and 4 and of eq 3 and 5 gives

$$k_p = \sum_i^r \sum_j^m k_{ij}p_if_j \tag{8}$$

$$k_t = \sum_i^r \sum_j^r k_{tij}p_ip_j \tag{9}$$

where p_i and f_j are the relative concentrations given by

$$p_i = [P_i\cdot]/[P\cdot] \tag{10}$$

$$f_j = [M_j]/[M] \tag{11}$$

with $\sum p_i = \sum f_j = 1$.

We now assume that (i) the produced chains are long enough and (ii) one type of radical changes to another fast enough compared with the initiation and termination reactions so that the effects of the chain ends are unimportant. Then, each growing chain and hence the system as a whole may be viewed as being in the *stationary state* in which the relative concentrations of the radicals are constant, being defined only by the mechanism of the propagation step and the composition of the feed. More specifically, the assumption of stationarity generally gives $r - 1$ simultaneous equations to solve for p_i's as a function of the relevant rate constants and the feed composition only. All we are saying is that in this state, k_p and k_t as well as the copolymer composition are constant for a given composition of the feed, being independent of other factors such as the total radical concentration and chain length. In this context, the rate equations for copolymerization are formally the same as those for homopolymerization.

In the steady state in which [P·] as well as p_i's are constant, we may equate R_i to R_t to obtain the familiar relation

$$R_p = (k_p/k_t^{1/2})R_i^{1/2}[M] \quad (12)$$

Thus by measuring R_i and R_p (in the present treatments, R_p may be identified with the polymerization rate) for a given composition of the feed, we have the ratio ω defined by

$$\omega = k_p/k_t^{1/2} \quad (13)$$

Insofar as k_p and k_t are constant for a constant composition of the feed, the rotating-sector equation for copolymerization is obviously the same as that for homopolymerization. If we let R_{pL} and R_{pD} be the rates of steady-state polymerization in the light and dark, respectively, the average rate $\bar{R}_p$ under the intermittent illumination with light time t_L and dark time t_D is related to the radical lifetime τ_L by

$$\bar{R}_p/R_{pL} = (s + 1)^{-1}[(sy + 1) + b^{-1} \ln (Z/8y)] \quad (14a)$$

$$Z = (1 + A_1A_2)(1 + y)^2 - (A_1 + A_2)(1 - y)^2 + \{[(1 + A_1A_2)(1 + y)^2 - (A_1 + A_2)(1 - y)^2]^2 - 64A_1A_2y^2\}^{1/2} \quad (14b)$$

where $A_1 = \exp(-2b)$ and $A_2 = \exp(-2bsy)$ with $b = t_L/\tau_L$, $y = R_{pD}/R_{pL}$, and $s = t_D/t_L$. Equation 14 is equivalent to but somewhat simpler in form than the conventionally used equation.[43] The lifetime τ_L is related to the rate constants by the familiar relation

$$\tau_L R_{pL}/[M] = k_p/k_t \quad (15)$$

As in the case of homopolymerization, the combination of the steady- and non-steady-state experiments yields individual values of k_p and k_t.

Terminal Model. This classical model distinguishes only the two types of radicals, one carrying monomer 1 at the growing end, and the other, monomer 2, and assumes no other complication. The stationary-state assumption yields the well-known expressions for the radical population p_1 (=1 − p_2), the copolymer composition F_1 (=1 − F_2), and the rate constant k_p:

$$k_{12}p_1f_2 - k_{21}p_2f_1 = 0 \quad (16)$$

$$\frac{F_1}{F_2} = \frac{f_1(r_1f_1 + f_2)}{f_2(r_2f_2 + f_1)} \quad (17)$$

$$k_p = \frac{r_1f_1^2 + 2f_1f_2 + r_2f_2^2}{(r_1f_1/k_{11}) + (r_2f_2/k_{22})} \quad (18)$$

where $r_i = k_{ii}/k_{ij}$ ($i \neq j$) is the reactivity ratio, and k_{ij} is the rate constant for the radical i to add monomer j (i, j = 1 or 2). According to this model, all four k_{ij}'s should be independent of the ω:[8] composition f_1 (=1 − f_2), and thus the propriety of the model must be evaluated with respect to both eq 17 and 18. The latter equation, however, has never been critically tested, as already stated.

Insofar as the mechanism of the termination reaction is unknown, the steady-state polymerization parameter ω (eq 13) by itself provides no information about the validity of the terminal model. If the termination step is assumed to be characterized only by the above two types of radicals, the termination rate constant may be generally represented by (see eq 9)

$$k_t = k_{t11}p_1^2 + 2k_{t12}p_1p_2 + k_{t22}p_2^2 \quad (19)$$

with p_1 (=1 − p_2) given by eq 16. In the chemically controlled termination model of Walling, all k_{tij}'s are independent of f_1, and thus k_{tii} is equal to the rate constant for the relevant homopolymerization. The combination of eq 18 and 19 yields the well-known expression for ω:[8]

$$\omega = (r_1f_1^2 + 2f_1f_2 + r_2f_2^2)/[(r_1f_1/\omega_1)^2 + (2r_1r_2f_1f_2/\omega_1\omega_2)\phi + (r_2f_2/\omega_2)^2]^{1/2} \quad (20)$$

$$\omega_i = k_{ii}/k_{tii}^{1/2} \qquad i = 1 \text{ or } 2 \quad (21)$$

$$\phi = k_{t12}/(k_{t11}k_{t22})^{1/2} \quad (22)$$

In the diffusion-controlled termination model of Atherton and North,[9] it is assumed that $k_{t11} = k_{t22} = k_{t12} = k_t$, where k_t is considered to be a function of the physical properties of the growing chain and its environment: the "ideal" termination model was defined by[9]

$$k_t = F_1k_{t1} + F_2k_{t2} \quad (23)$$

where k_{ti}'s refer to the homopolymerizations. The explicit expression for ω is obtained by inserting eq 18 and 23 in eq 13.

As already stated, most copolymerizations exhibit large, composition-dependent values of ϕ, indicating the failure of eq 20. This characteristic behavior cannot be comprehensively interpreted by the diffusion model either. Thus far, this problem has been discussed only in the realm of the termination step, and more sophisticated termination models have been proposed.[6,10-13] However, the alternative view that the problem may be concerned with the propagation step should not be ruled out.

Volume Contraction Factor. In rotating-sector experiments, polymerization rates are determined usually by the dilatometric method, which requires accurate knowledge of the contraction factor Γ, i.e., the volume decrease per unit mole of the monomers polymerized. We have pointed out the inadequacy of the conventional methods for estimating this factor and on the basis of the van Laar–Scachard type equation of mixing derived the following expression for Γ° (in mL mol^{-1}) for an incipient copolymerization in the bulk[44] (see note 45):

$$\Gamma^\circ = (F_1\Gamma_1^\circ + F_2\Gamma_2^\circ)(1 - a_{12}x_1x_2) - F_{12}\Delta V_{12} + x_2F_1(a_{12}V_1 + \tilde{V}_{1,1}^\circ - \tilde{V}_{1,2}^\circ) + x_1F_2(a_{12}V_2 + \tilde{V}_{2,2}^\circ - \tilde{V}_{2,1}^\circ) \quad (24)$$

$$\Gamma_i^\circ = V_i - \tilde{V}_{i,i}^\circ \qquad i = 1 \text{ or } 2 \quad (25)$$

Here the superscript degree denotes the infinite dilution, V_i is the molar volume of pure monomer i, $\tilde{V}_{i,j}^\circ$ is the partial molar volume of polymer i (per monomeric unit) in monomer j, and x_i is the volume fraction of monomer i before mixing: $x_1 = 1 - x_2 = f_1V_1/(f_1V_1 + f_2V_2)$. Furthermore, the parameter a_{12} is related to the excess volume of mixing the monomers

$$V_s = (f_1V_1 + f_2V_2)(1 + a_{12}x_1x_2) \quad (26)$$

where V_s is the molar volume of the mixture. The parameter ΔV_{12} is defined as the excess volume of the formation of 1–2 chemical bonds, and it can be determined experimentally on the basis of the equation

$$\tilde{V}_{p,j}^\circ = F_1\tilde{V}_{1,j}^\circ + F_2\tilde{V}_{2,j}^\circ + F_{12}\Delta V_{12} \quad (27)$$

where $\tilde{V}_{p,j}^\circ$ is the partial molar volume (per monomeric unit) of a copolymer, and F_{12} is the population of 1–2 chemical bonds. The adequacy of eq 24 has been experimentally verified elsewhere.[42,44]

Experimental Section

Materials. Commercial products of ST and MMA were purified according to the standard methods.[3] 2,2′-Azobis(isobutyronitrile) (AIBN) and 2,2′-azobis(cyclohexane-1-carbonitrile) (ACN) purchased from Nakarai Chemicals, Japan, and 4-hydroxy-2,2,6,6-tetramethylpiperidinyl-1-oxy (HTMPO) from

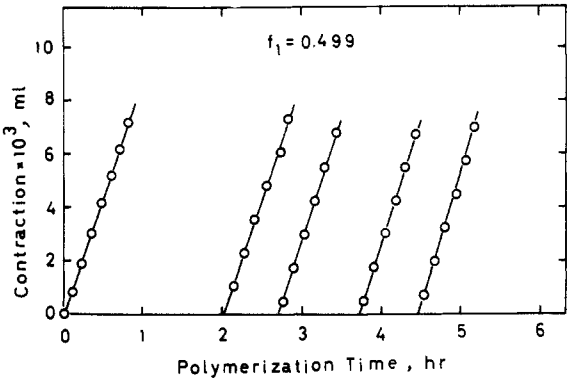

Figure 1. Plot of volume contraction vs. polymerization time for ST/MMA/AIBN/HTMPO/40 °C systems with $f_1 = 0.499$ and $10^2 \times$ [HTMPO]/[AIBN] = 0, 0.429, 0.564, 0.735, and 0.894 (from left to right).

Table I
Values of the Volumetric Parameters in Eq 24 for the Copolymerization of ST(1) and MMA(2) at 40 °C[a]

V_1	117.04	$\tilde{V}_{1,1}°$	96.51
V_2	108.61	$\tilde{V}_{1,2}°$	96.41
$10^3 A_0$[b]	−2.9	$\tilde{V}_{2,1}°$	80.90
$10^3 A_1$[b]	−3.2	$\tilde{V}_{2,2}°$	81.20
ΔV_{12}	−1.42		

[a] V's and ΔV_{12} are in mL mol^{-1}. [b] $a_{12} = A_0 + A_1(x_1 - x_2)$.

Eastman Kodak, Rochester, NY, were recrystallized from an ethanol solution (for AIBN and ACN) or a petroleum ether solution (for HTMPO), dried in a vacuum oven, and kept in a refrigerator (−20 °C) until required.

Steady-State Polymerization. A known amount of the initiator AIBN was charged in a Pyrex tube equipped with a three-way tap, through which ST and then MMA were syringed in under a nitrogen atmosphere. At each stage, the tube plus fittings were weighed to determine the monomer weights charged. The tube was then connected by a rubber tube to a vacuum line and degassed with freezing–thawing cycles repeated (usually 7–10 cycles) until no bubbles were formed in the mixture. Finally, the tube was sealed off under vacuum. It was confirmed that no significant weight loss was caused by degassing. The value of f_1 determined in this way is estimated to be correct to less than 0.3% for all compositions.

The mixture thus prepared was allowed to polymerize at 40 °C in a water bath equipped with a shaker. Polymerization was terminated by quenching in liquid nitrogen. The precipitate from a 30-fold excess of methanol was dried to a constant weight and weighed to determined the conversion. The polymer was further purified by precipitation from a benzene solution into methanol and subjected to the molecular characterization: The copolymer composition was determined by combustion analysis for carbon. The number- and weight-average molecular weights, M_n and M_w, were estimated by gel permeation chromatography (GPC) with the column system calibrated with standard PST's and PMMA's. It was assumed that the calibration curve for a copolymer is given by the composition average of those for the homopolymers. Reagent grade tetrahydrofuran was used as a carrier solvent.

The initiation rate was determined by the inhibitor method. According to the same procedure as above, known amounts of AIBN, HTMPO (inhibitor), and the monomers were charged in a Pyrex tube to which two Pyrex dilatometers were connected. The solution, thoroughly degassed and sealed off under vacuum, was poured into the dilatometers to fill them to a predetermined level. In this way, it was possible to duplicate measurements under the same condition. The inhibition time was determined at 40 °C by visually following the meniscus level. Typical examples of the level vs. time curves are presented in Figure 1. In these and all other cases examined, the plot was linear after the onset of polymerization to yield a well-defined inhibition time.

Volume Contraction Factor. All the parameter values included in eq 24 were individually determined by measuring the densities of appropriate solutions.[42] Numerical results are listed in Table I. The value of $\Gamma°$ computed from eq 25 with these parameter values should be correct to ±1% for all compositions.[42]

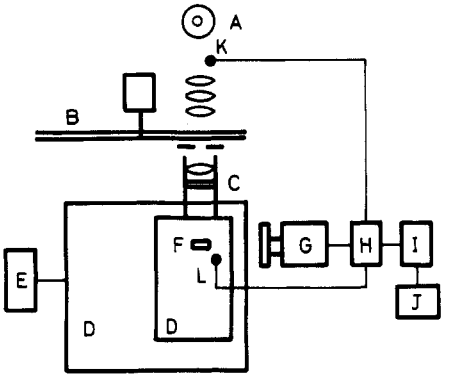

Figure 2. Block diagram of the rotating-sector system: A, light source; B, rotating sectors; C, optical filter; D, double water bath; E, thermoregulater; F, sample cell; G, detector camera; H, AD converter; I, microcomputer; J, printer; K, photodiode intensity monitor; L, thermistor.

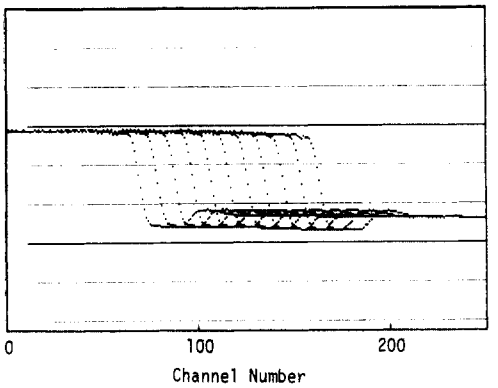

Figure 3. Display of the detector responses following the steady-state polymerization of a MMA/ACN/40 °C system (scanned 11 times at an interval of 30 s).

Non-Steady-State Polymerization. The radical lifetime was measured by the rotating-sector method. Figure 2 shows a block diagram of the apparatus used in this study. The radiation from a 400-W high-pressure mercury lamp (Toshiba H400-F, Japan), which was passed through a 365-nm filter (Toshiba UV-D36B, Japan), was used as a light source. The rotating sector, driven by a synchronous motor with appropriate reduction gears, consisted of two black-painted aluminum disks, 60 cm in diameter, with two rectangular sectors cut out in symmetrical positions so as to give an arbitrary dark-to-light ratio s when the two disks are combined ($s = 2$ in this study). A double water bath with the outer bath thermoregulated to about ±0.01 °C was employed. The temperature variation in the inner (sample) bath, which was monitored by a thermistor circuit, was less than 0.001 °C during one rate experiment (usually, 10–20 min). Drum-shaped Pyrex cells of ca. 10-mL capacity connected to a capillary of ca. 1.25-mm inside diameter were used as dilatometers, which were charged with ACN (photosensitizer) and the monomers according to the same procedure as for the inhibition time experiment.

The meniscus level of the reaction mixture was followed automatically by the image sensor system which we recently developed in collaboration with Unisoku Co. Ltd., Hirakata, Japan. The system consists of a camera, an interface, and a microcomputer: The image of the meniscus, enlarged by a factor about 1.5, is projected on a diode-array detector FX-100 (Flex Co. Ltd., Osaka, Japan) which is set in the camera. The detector, consisting of 1024 photodiode elements in an array, has a sensitive area of 28 × 0.5 mm and a scanning velocity of 10 ms. The electric signal from each element is transferred through an AD converter to the microcomputer which carries out necessary operations and calculations. An example of the graphic display of detector responses is presented in Figure 3, in which the intensities detected by 250 diode elements are plotted against the channel number. The horizontal distance between two adjacent points in the display corresponds to about 20 μm on the capillary scale. In this example,

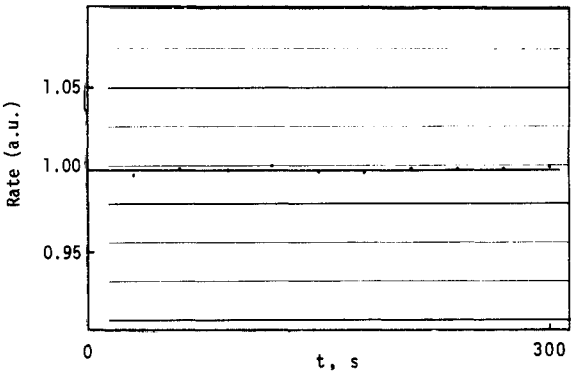

Figure 4. Rate of meniscus migration plotted against time (data from Figure 3).

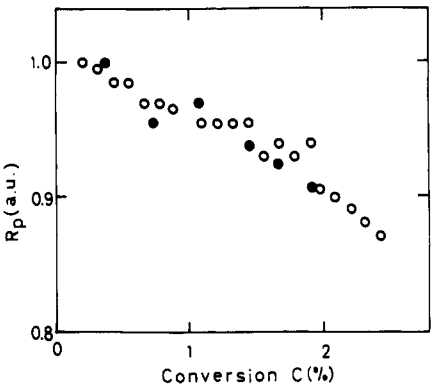

Figure 5. Plot of R_p vs. C for ST/ACN/40 °C systems, illuminated (filled circles) and not illuminated (open circles).

the steady-state polymerization of MMA was followed by scanning 11 times at a 30-s interval. The leftward migration of the entire plot indicates a descent of the meniscus. This set of data is appropriately manipulated by the computer, and we have the rate of meniscus migration for every 30 s, as shown in Figure 4. In this example, the standard deviation for the measurement of a 200-μm migration is estimated to be about 1 μm (0.5%). Presumably, this degree of accuracy will be difficult to achieve by visual observation. Also importantly, the present system does emancipate us from the laborious and skill-requiring work of visual observation.

During the course of preliminary experiments with this system, it was noted that the steady-state rate R_p varies significantly with the conversion C even in a low C region. In Figure 5, R_p is plotted against C for the polymerization of ST initiated by ACN. The figure shows that R_p monotonously decreases as C increases up to about 2%, regardless of the system being illuminated or not. A similar dependence was observed in all the examined homo- and copolymerizations of ST and MMA initiated by ACN and also by AIBN. Qualitatively the same results have been reported in the literature,[46,47] and this phenomenon seems general rather than exceptional. This poses a rather serious problem on the lifetime evaluation, for it is quite difficult to carry out a series of sector experiments in a C region low enough for the C dependence of R_p to be negligible.

We have dealt with our data according to two methods: In method 1, (a) R_{pL} is measured before and after each sector run to estimate, by interpolation, the R_{pL} value corresponding to the sector run, (b) no correction is given to the t_L axis of the $\bar{R}_p/R_{pL}$ vs. log t_L plot, and (c) the algebraic average $\langle R_{pL} \rangle$ of the series of R_{pL} data is used to evaluate k_p/k_t according to eq 15. The k_p/k_t ratio thus obtained should be regarded as a certain, though poorly defined, average over the relevant C region, and may possibly be compared to the $k_p/k_t^{1/2}$ ratio obtained by the batch experiment carried out in a similar C region. Method 2 is the same as method 1 except for the point (b) and is based on the plausible assumption that k_t, rather than k_p and R_i, depends on C.[48] Elimination of k_t from eq 12 and 15 gives

$$\tau_L/R_{pL} = \tau_{L,0}/R_{pL,0} = \text{constant} \quad (28)$$

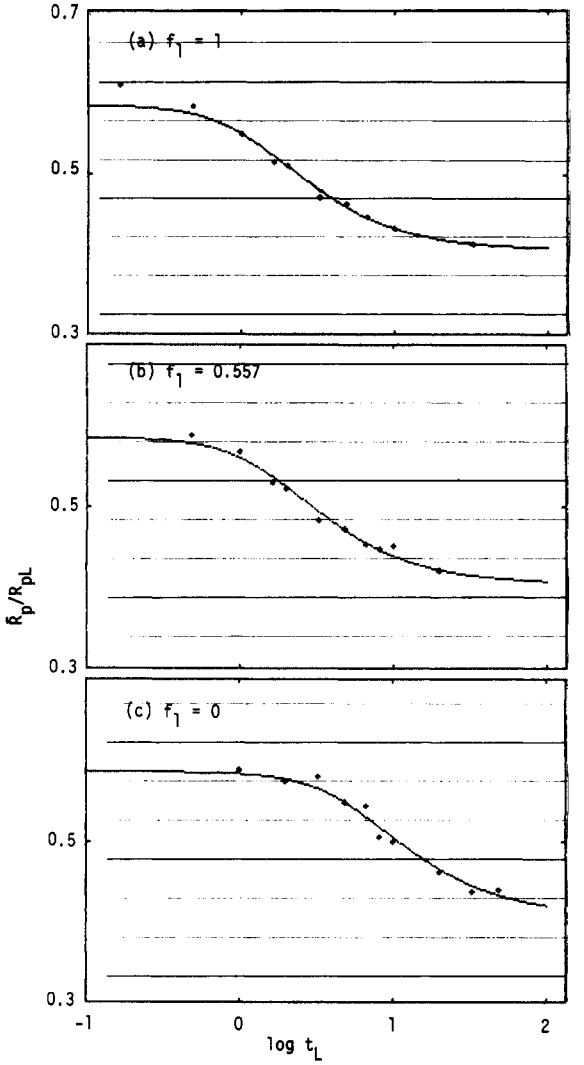

Figure 6. Plot of $\bar{R}_p/R_{pL}$ vs. log t_L for ST/MMA/ACN/40 °C systems for $t_D/t_L = 2$: (a) $f_1 = 1$, [ACN] = 7.66×10^{-3} mol L^{-1}, and $y = R_{pD}/R_{pL} = 0.108$; (b) $f_1 = 0.577$, [ACN] = 7.09×10^{-3}, and $y = 0.106$; (c) $f_1 = 0$, [ACN] = 0.795×10^{-3}, and $y = 0.111$.

where the subscript 0 denotes an arbitrary reference state. The ratio $\bar{R}_p/R_{pL}$, which is a function of $b = t_L/\tau_L$, plotted against $t_L' = (R_{pL,0}/R_{pL})t_L$ then becomes independent of C and gives the value of $\tau_{L,0}$. By setting $R_{pL,0}$ equal to the algebraic average $\langle R_{pL} \rangle$, we calculated the values of k_p/k_t by both methods 1 and 2 and found that the two methods result in differences smaller than a few percent in most cases. Thus, it will suffice to consider results obtained by method 1, which includes no assumption.

Figure 6 shows typical examples of the $\bar{R}_p/R_{pL}$ vs. log t_L plot obtained for the homo- and copolymerizations of ST and MMA. An appropriate correction was made for the variation of the intensity of the light source monitored by a photodiode circuit. The solid lines in the figure were computed with eq 14 by a least-squares curve-fitting method. It may be seen that the copolymerization as well as the homopolymerizations are well represented by eq 14. The error associated with the determination of lifetime was estimated to be about ±10% for all compositions.

Results and Discussion

All copolymerization runs were carried out at conversions less than 3% by weight so that composition drifts with conversion may be neglected. Results of the steady-state polymerization with AIBN initiator are listed in Table II. The molecular weights of the steady-run samples, as estimated by the GPC analysis, are included in the same table. The values of M_n are of the order 10^5, apparently large enough for the long-chain approximations

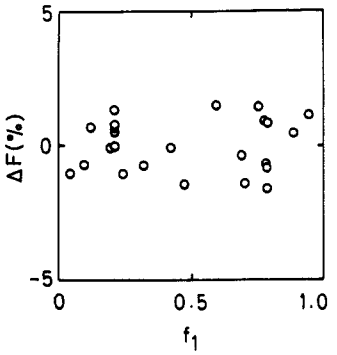

Figure 7. Residuals $\Delta F = F_{obsd} - F_{calcd}$ plotted against f_1 for the ST–MMA copolymers obtained by the AIBN-initiated bulk polymerization in ampule.

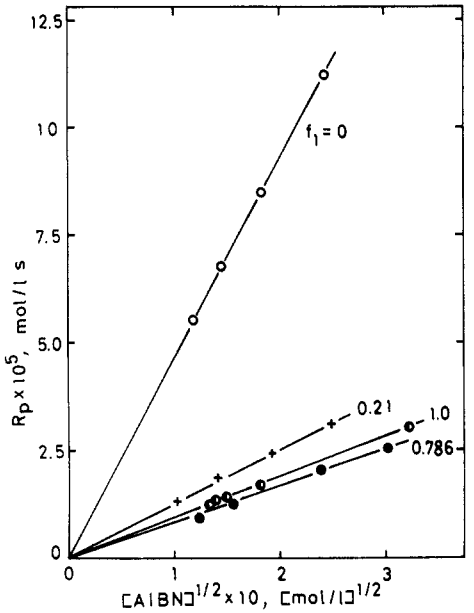

Figure 8. Plot of R_p vs. $[AIBN]^{1/2}$ for ST/MMA/AIBN/40 °C systems.

to be applicable. The M_w/M_n ratios range between 1.5 and 2.0, as is typical of polymers produced by "normal" mechanisms of free-radical polymerization.[48] The values of M_n of the sector-run samples were also found to be large enough, while their M_w/M_n ratios were, as expected, considerably larger than those of the steady-run samples of comparable composition (cf. Table IV).

The composition data presented in Table II were fitted to the terminal-model eq 17 by the method of least squares[3] to yield $r_1 = 0.523$ and $r_2 = 0.460$ as optimum reactivity ratio values. These are close to literature values.[49] In Figure 7, the residual $\Delta F = F_{obsd} - F_{calcd}$ is plotted against f_1, where F_{obsd} is the observed composition of ST, and F_{calcd} is that calculated with the terminal model with the optimum r_1 and r_2 values. Apparently, the data points are distributed within the range of analytical uncertainty (about ±1.5%), showing no systematic trend. This confirms the previous conclusion that the composition of this system conforms to the terminal model within experimental error. We also note that the compositions of the sector-run samples were found to be perfectly consistent with the above F–f relation (cf. Table IV).

In Figure 8, the steady-state polymerization rate R_p is plotted against the square root of the initiator concentration. In all examined cases, R_p is proportional to $[AIBN]^{1/2}$ within experimental error.

In Figure 9, the inhibition time t_i is plotted against the concentration ratio of inhibitor to initiator, [HTMPO]/[AIBN]. In all examined cases, proportionality held between these quantities. The values of $2fk_d$ determined from the slopes of the plot are given in Table III and

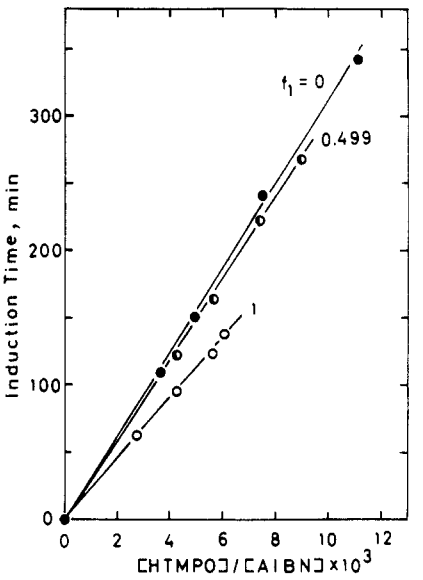

Figure 9. Plot of induction time vs. inhibitor-to-initiator concentration ratio for ST/MMA/AIBN/HTMPO/40 °C systems.

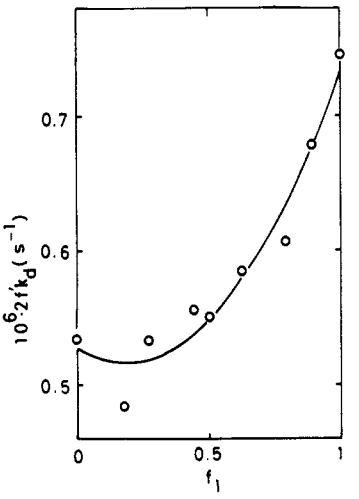

Figure 10. Plot of $2fk_d$ vs. f_1 for the ST/MMA/AIBN/40 °C system.

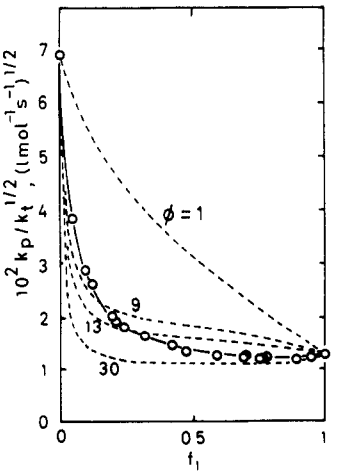

Figure 11. Plot of $\omega = k_p/k_t^{1/2}$ vs. f_1 for the ST/MMA/40 °C system. The solid curve is the best-fit representation of the experimental data (open circles), while the broken curves represent the Walling eq 20 with the values of ϕ indicated in the figure.

Table II
Summary of the Batch Copolymerization of ST and MMA in the Bulk at 40 °C

run	f_1[a]	[M],[b] mol/L	10^2[I],[c] mol/L	t,[d] min	Y,[e] wt %	F_1[f]	$10^4R_p/[I]^{1/2}$, $(mol/L)^{1/2}/s$	$10^{-5}M_n$[g]	M_w/M_n[g]
1	0	9.207	2.207	125	5.53	0.002	4.626[h]	6.94	1.87
2			1.413	120	4.32	−0.001			
3			3.364	90	4.98	−0.002		4.78	1.89
4			5.921	60	4.39	−0.004		3.63	1.83
5	0.046	9.174	1.891	60	1.38	0.078	2.554		
6	0.096	9.140	1.878	120	2.06	0.158	1.904	3.77	1.68
7	0.121	9.123	2.028	120	1.94	0.205	1.721	3.31	1.79
8	0.194	9.072	1.968	120	1.48	0.278	1.325		
9	0.210	9.062	1.067	180	1.59	0.300	1.246[h]	4.75	1.64
10			2.019	120	1.48	0.299		3.78	1.57
11			3.708	90	1.46	0.294			
12			6.202	90	1.85	0.301			
13			10.133		1.13	0.308			
14	0.241	9.041	1.928	120	1.31	0.312	1.181	4.30	1.57
15	0.319	8.988	1.783	300	2.87	0.378	1.071		
16	0.422	8.920	1.784	300	2.59	0.458	0.960	3.29	1.54
17	0.474	8.887	2.013	300	2.55	0.479	0.887	2.84	1.60
18	0.592	8.811	2.037	300	2.46	0.587	0.844	2.80	1.48
19	0.692	8.746	1.986	300	2.38	0.640	0.823	2.65	1.54
20	0.702	8.739	1.891	120	0.96	0.637	0.849		
21	0.756	8.704	1.748	300	2.27	0.710	0.832	2.56	1.51
22	0.774	8.691	1.895	300	2.39	0.720	0.840	2.79	1.50
23	0.786	8.684	1.156	150	0.95	0.714	0.855[h]	3.34	1.55
24			2.247	120	1.03	0.731		2.60	1.56
25			3.783	90	1.01	0.697			
26			5.729	60	0.85	0.706			
27			9.212	60	1.05	0.713			
28	0.832	8.655	1.614	120	0.88	0.791	0.834	2.89	1.52
29	0.891	8.616	2.046	300	2.50	0.838	0.838	2.60	1.56
30	0.944	8.581	1.967	300	2.59	0.922	0.882		
31	1	8.544	1.800	300	2.69	1.003	0.943[h]	2.82	1.45
32			2.245	300	3.01	1.001		2.58	1.48
33			1.930	635	5.98			2.37	1.54
34			3.303	523	6.24			1.92	1.54
35			10.515	186	4.00				

[a] Mole fraction of ST in feed. [b] Total monomer concentration. [c] AIBN concentration. [d] Reaction time. [e] Conversion. [f] Mole fraction of ST in copolymer. [g] GPC value. [h] Average value.

Figure 10. These data were fitted to a parabolic function of f_1 by a least-squares method to yield

$$2f'k_d = 0.329f_1^2 - 0.123f_1 + 0.528 \quad (\times 10^{-6}\ s^{-1}) \qquad (29)$$

On the basis of the steady-run data in Table II along with eq 29, the parameter $\omega = k_p/k_t^{1/2}$ was evaluated. It is plotted against f_1 in Figure 11. The solid curve in the figure is the best-fit representation of the data, which will be used for later analysis.

The radical lifetime was measured for 11 different values of f_1 including $f_1 = 0$ and 1, and the ratio k_p/k_t was determined for each composition. With these and the ω data, k_p and k_t were individually evaluated as a function of f_1. Tables IV and V show the results. The rate constant values are expected to be correct to about 20% for k_p and about 40% for k_t, for all values of f_1. Reported values of k_p and k_t for both ST and MMA are so largely different among themselves that comparison with them may be pointless. Nevertheless, we note that our values are, for both ST and MMA, approximately equal to the algebraic averages of the literature values.[50]

We now have a complete set of data to test the propriety of kinetic models. By using the experimental values of k_p for the homopolymerizations (k_{11} = 120 and k_{22} = 377 L mol^{-1} s^{-1}) and of r_1 and r_2, we calculate the values of k_p predicted by the terminal model, eq 18, which is shown by the broken curve in Figure 12. Alternatively, we solve eq 13 for k_t by using the experimental value of ω and the terminal-model value of k_p. The open circules in Figure 13 represent the k_t calculated in this way. These predictions by the terminal model are utterly at variance with

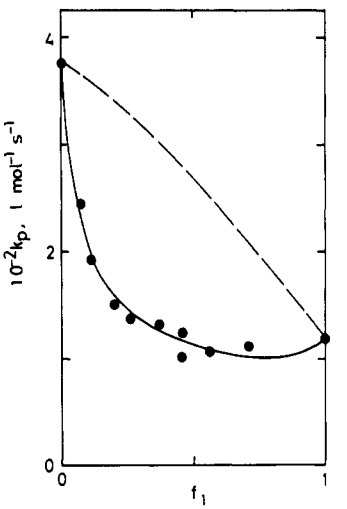

Figure 12. Plot of k_p vs. f_1 for the ST/MMA/40 °C system: the filled circles were measured, and the broken curve was calculated with the terminal model (eq 18 with r_1 = 0.523, r_2 = 0.460, k_{11} = 120 L mol^{-1} s^{-1}, and k_{22} = 377 L mol^{-1} s^{-1}). The solid curve is the best-fit representation by the penultimate model (eq 30–32 with $r_1 = r_1' = 0.523$, $r_2 = r_2' = 0.460$, k_{111} = 120 L mol^{-1} s^{-1}, k_{222} = 377 L mol^{-1} s^{-1}, s_1 = 0.30, and s_2 = 0.53).

the experimental data, shown by the filled circles in Figures 12 and 13. For a certain range of f_1, the calculated values of k_t are larger than the observed values by a factor exceeding 5, much too large to be explained in terms of experimental artifacts. We thus unequivocally conclude that the terminal model entirely fails to represent the

Table III
Inhibition Times of the ST/MMA/AIBN/HTMPO System (40 °C)

f_1[a]	10^2[AIBN], mol/L	10^4[HTMPO], mol/L	t_i,[b] min	$10^6(2fk_d)$,[c] s^{-1}
0	8.049	2.927	109	0.535
	8.229	4.080	151	
	7.715	5.774	241	
	8.611	9.576	342	
0.180	8.700	3.343	123	0.484
	8.251	4.324	178	
	8.251	5.645	236	
0.273	6.903	2.905	128	0.534
	6.931	4.209	182	
	6.831	5.022	227	
	7.096	6.766	299	
0.442	7.698	3.436	138	0.556
	7.661	5.135	197	
	8.001	6.720	253	
0.499	7.046	3.022	122	0.551
	7.457	4.204	164	
	7.658	5.628	224	
	7.813	6.987	268	
0.627	7.833	3.016	99	0.585
	7.622	4.535	157	
	7.434	6.325	236	
	7.312	7.573	295	
0.792	7.363	2.509	84	0.607
	7.270	3.991	143	
	7.114	6.864	264	
0.893	7.496	3.153	112	0.679
	7.557	4.396	146	
	7.512	7.383	242	
1	9.053	2.481	62	0.746
	2.025	0.868	95	
	2.299	1.391	138	
	8.698	4.892	123	

[a] Mole fraction of ST. [b] Inhibition time. [c] Average value.

propagation rate of the ST–MMA system.

Also to be noted is the magnitude of the observed values of k_t. At all compositions, the copolymerization k_t is between the two homopolymerization values. The present system has been believed to have large, composition-dependent values of ϕ. In agreement to previous results,[8,15-19] the open circles in Figure 13 correspond to values of ϕ ranging from about 9 to about 30 (in order of increasing f_1). It is now clear that the large ϕ is a direct consequence of applying the erroneous model for the propagation step. The true ϕ is close to unity for all compositions, as is indicated by the broken curve in Figure 13 which represents eq 19 with $\phi = 1$ (see note 51). This result is consistent with what is predicted from the behavior of low

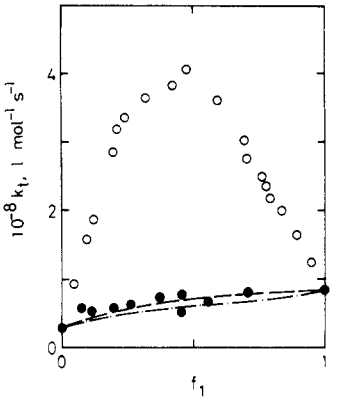

Figure 13. Plot of k_t vs. f_1 for the ST/MMA/40 °C system: the filled circles were measured and the open circles were calculated from the experimental values of $\omega = k_p/k_t^{1/2}$ (Figure 11) and the terminal-model values of k_p (eq 18: the broken curve in Figure 12). The broken curve represents eq 19 with $\phi = 1$, and the dot–dash curve represents the diffusion model, eq 23.

molecular weight radicals, on the one hand, and from the theoretical calculation by means of the molecular orbital method,[52] on the other.

However, the fact that the $\phi = 1$ model closely represents the experimental data does not necessarily imply a chemically controlled termination. The diffusion model, eq 22, also describes the data quite well (dot–dash curve, Figure 13), and it seems difficult to choose between the two by numerical comparison alone. In view of the body of evidence[53-56] suggesting that diffusion rather than chemistry is the rate-determining factor in polymer radical systems, the diffusion model may be more realistic.

In any case, these results imply that the termination step in copolymerization obeys a simple rather than "unusual" rule: as far as numerical values are concerned, it is well represented by the $\phi = 1$ model. If this implication is correct, it follows that the failure of the terminal model is general rather than exceptional, since, as already noted, most systems exhibit large values of ϕ according to the conventional analysis based on that model. The need is apparent for reexamining other systems with respect to the absolute values of the individual rate constants.

Finally, some words are due regarding the mechanism of the propagation step. Typical models so far proposed as an alternative for the terminal model include the penultimate model,[4] the monomer–monomer complex model,[57] the hot radical model,[58] and the radical–solvent complex model.[59] As to the ST–MMA system, the penultimate

Table IV
Summary of the Lifetime Measurements for the Copolymerization of ST and MMA at 40 °C and the Characteristics of the Recovered Polymers

f_1[a]	10^3[ACN], mol/L	$10^5\langle R_{pL}\rangle$, (mol/L)/s	$R_{pD}/\langle R_{pL}\rangle$	τ_L, s	polymer characteristics		
					F_1[b]	$10^{-5}M_n$[c]	M_w/M_n[c]
0	0.648	2.672	0.122	4.60			
	0.795	3.016	0.111	3.59			
	0.822	3.007	0.117	4.02		11.21	3.41
0.073	5.273	3.389	0.114	1.12	0.118 (0.132)	6.63	1.71
0.109	7.965	2.980	0.114	1.10	0.184 (0.183)	4.59	3.28
0.199	7.945	2.271	0.108	1.07	0.284 (0.284)	4.20	2.86
0.262	8.063	1.811	0.129	1.12	0.340 (0.341)	3.91	2.77
0.377	7.945	1.718	0.109	0.90	0.402 (0.428)	3.54	2.46
0.454	8.246	1.447	0.120	1.23			
0.458	8.884	1.601	0.120	0.87	0.489 (0.483)	3.07	3.01
0.557	7.087	1.386	0.106	0.99	0.544 (0.548)	3.00	3.28
0.705	9.583	1.363	0.106	0.89	0.643 (0.654)	2.92	2.53
1	7.661	1.484	0.108	0.78		3.05	3.10
	7.989	1.642	0.099	0.75			

[a] Mole fraction of ST in feed. [b] Mole fraction of ST in copolymer. The value in parentheses was calculated. [c] GPC value.

Table V
Values of the Rate Constants of Propagation and Termination for the Bulk Copolymerization of ST and MMA at 40 °C

f_1[a]	$10^2 k_p/k_t^{1/2}$,[b] $[(L/mol)/s]^{1/2}$	$10^5 k_p/k_t$[c]	k_p, (L/mol)/s	$10^{-6} k_t$, (L/mol)/s
0	6.92	1.34	359	27
		1.18	407	35
		1.31	365	28
0.073	3.20	0.414	247	60
0.109	2.63	0.359	193	54
0.199	2.00	0.268	149	56
0.262	1.77	0.225	139	62
0.377	1.53	0.173	135	78
0.454	1.42	0.200	101	50
0.458	1.41	0.156	127	82
0.557	1.30	0.155	109	70
0.705	1.23	0.138	110	79
1	1.29	0.135	123	91
		0.144	116	80

[a] Mole fraction of ST in feed. [b] Value read from the solid curve in Figure 11. [c] From the rotating-sector experiments.

model may be suggested by the fact that the addition of various solvents to the system does not change the essential features of the R_p vs. f_1 curve.[11,19]

It may be convenient to express the propagation rate constant in the following general form:

$$k_p = \frac{\bar{r}_1 f_1^2 + 2f_1 f_2 + \bar{r}_2 f_2^2}{(\bar{r}_1 f_1/\bar{k}_{11}) + (\bar{r}_2 f_2/k_{22})} \quad (30)$$

where $\bar{r}_i$ and $\bar{k}_{ii}$ are constant for the terminal model (cf. eq 18) but generally, functions of the composition of feed. For the penultimate model, they read

$$\bar{r}_1 = \frac{r_1'(f_1 r_1 + f_2)}{f_1 r_1' + f_2} \qquad \bar{r}_2 = \frac{r_2'(f_2 r_2 + f_1)}{f_2 r_2' + f_1} \quad (31)$$

$$\bar{k}_{11} = \frac{k_{111}(r_1 f_1 + f_2)}{r_1 f_1 + (f_2/s_1)} \qquad \bar{k}_{22} = \frac{k_{222}(r_2 f_2 + f_1)}{r_2 f_2 + (f_1/s_2)} \quad (32)$$

with

$$r_i = k_{iii}/k_{iij} \quad (i \neq j) \quad (33)$$

$$r_i' = k_{jii}/k_{jij} \quad (i \neq j) \quad (34)$$

$$s_i = k_{jii}/k_{iii} \quad (i \neq j) \quad (35)$$

where k_{pmn} is the rate constant for the radical with a terminal unit m and a penultimate unit p to add a monomer n ($p, m, n = 1$ or 2). Since the composition curve of the ST–MMA system is well represented by the terminal model (see above), we may assume that $r_1 = r_1'$, and $r_2 = r_2'$. Then s_1 and s_2 are the only unknowns included in the model. A least-squares curve-fitting calculation yielded $s_1 = 0.30$, and $s_2 = 0.53$ as optimum values. The solid curve in Figure 12 shows eq 30 with these parameter values. It satisfactorily represents the experimental points, indicating that the penultimate model is useful at least as a phenomenological model. However, we should await more experimental and theoretical work before a definite conclusion about the model propriety is reached.

Acknowledgment. We thank Professor M. Kinoshita, Osaka City University, for his kind help on our work. We also thank Professor M. Imoto, Kansai University, Professor M. Kamachi, Osaka University, and Dr. K. Ito, Government Industrial Research Institute, Nagoya, for their interest in and valuable comments on this work.

Registry No. ST, 100-42-5; MMA, 80-62-6.

References and Notes

(1) A brief account of this paper has been presented in the following communication and symposium preprints. Because of a simple arithmetic mistake, the preliminary data on k_p and k_t therein illustrated for both the homo- and copolymerization of ST and MMA are incorrect: they are smaller than the correct values given in this paper by a constant factor of 4/5 for k_p and 16/25 for k_t. The arguments and conclusions therein presented need be modified in no essential point, however. (a) Fukuda, T.; Ma, Y.-D.; Inagaki, H. *Polym. Bull.* **1983**, *10*, 288. (b) Fukuda, T.; Ma, Y.-D.; Inagaki, H. *Polym. Prepr., Jpn.* **1983**, *32*, 1124, 1127. (c) Fukuda, T.; Ma, Y.-D.; Inagaki, H. 1st SPSJ International Polymer Conference, Kyoto, Japan, 1984, Abstract No. 22A11.
(2) Mayo, F. R.; Lewis, F. M. *J. Am. Chem. Soc.* **1944**, *66*, 1954.
(3) Fukuda, T.; Ma, Y.-D.; Inagaki, H. *Polym. J.* **1982**, *14*, 705.
(4) Merz, E.; Alfrey, T.; Goldfinger, G. *J. Polym. Sci.* **1946**, *1*, 75.
(5) Hill, D. J. T.; O'Donnell, J. H.; O'Sullivan, P. W. *Macromolecules* **1982**, *15*, 960.
(6) Ito, K.; O'Driscoll, K. F. *J. Polym. Sci., Polym. Chem. Ed.* **1979**, *17*, 3913.
(7) In ref 6, the rate constants of propagation and termination for a copolymerization system were individually determined by measuring the radical lifetimes. The following papers also deal with the measurements of the radical lifetimes in copolymerization systems, but the test of the terminal model is not the concern of these papers: (a) North, A. D.; Postlethwaite, D. *Trans. Faraday Soc.* **1966**, *62*, 2843. (b) Marano, J. P., Jr.; Shendalman, L. H.; Walker, C. *J. Polym. Sci., Part A-1* **1970**, *8*, 3461. (c) Kucher, R. V.; Anisimova, L. N.; Zaitsev, Yu. S.; Lachinov, M. B.; Zubov, V. P. *Vysokomol. Soedin., Ser. A* **1978**, *A20*, 2488. (d) Bamford, C. H.; Malley, P. J. *J. Chem. Soc., Faraday Trans. 1* **1982**, *78*, 2497.
(8) Walling, C. *J. Am. Chem. Soc.* **1949**, *71*, 1930.
(9) Atherton, J. N.; North, A. M. *Trans. Faraday Soc.* **1962**, *58*, 2049.
(10) Arlman, E. J. *J. Polym. Sci.* **1955**, *17*, 375.
(11) Bonta, G.; Gallo, B. M.; Russo, S. *J. Chem. Soc., Faraday Trans. 1* **1975**, *71*, 1727.
(12) Chiang, S. S. M.; Rudin, A. *J. Macromol. Sci., Chem.* **1975**, *A9*, 237.
(13) Prochazka, O.; Kratochvil, P. *J. Polym. Sci., Polym. Chem. Ed.* **1983**, *21*, 3269.
(14) Wittmer, P. *Makromol. Chem., Suppl.* **1979**, *3*, 129.
(15) Melville, H. W.; Valentine, L. *Proc. R. Soc. London, Ser. A* **1950**, *A200*, 337, 358.
(16) Bevington, J. C.; Melville, H. W.; Taylor, R. P. *J. Polym. Sci.* **1954**, *14*, 463.
(17) Suzuki, M.; Miyama, H.; Fujimoto, S. *J. Polym. Sci.* **1959**, *37*, 533.
(18) Kuan, H. U.; Wadehra, B. M. L. *Polymer* **1981**, *22*, 488.
(19) Madruga, E. L.; San Roman, J.; del Puetro, M. A. *Polymer* **1981**, *22*, 951.
(20) Horie, K.; Mita, I.; Kambe, H. *J. Polym. Sci.* **1969**, *7*, 2561.
(21) Walling, C.; McElhill, E. A. *J. Am. Chem. Soc.* **1951**, *73*, 2819.
(22) Chaudhuri, A. K.; Plait, S. R. *Makromol. Chem.* **1969**, *121*, 33.
(23) Burnett, G. M.; Evans, P.; Melville, H. W. *Trans. Faraday Soc.* **1953**, *49*, 1096, 1105.
(24) Ito, K. *J. Polym. Sci., Polym. Chem. Ed.* **1978**, *16*, 2725.
(25) Blanks, R. F.; Shah, B. N. *J. Polym. Sci., Polym. Chem. Ed.* **1976**, *14*, 2589.
(26) Pryor, W. A.; Hwang, T. L. *Macromolecules* **1969**, *2*, 70.
(27) Wittmer, P. *Angew. Makromol. Chem.* **1974**, *39*, 35.
(28) Fehervari, A.; Földes-Berezsnich, T.; Tüdös, F. *J. Macromol. Sci., Chem.* **1982**, *A18*, 347.
(29) Szafko, J.; Truska, E.; Lopatina, G. P. *Makromol. Chem.* **1975**, *176*, 2981.
(30) Arlman, E. J.; Melville, H. W. *Proc. R. Soc. London, Ser. A* **1950**, *A203*, 301.
(31) Bradbury, J. H.; Melville, H. W. *Proc. R. Soc. London, Ser. A* **1954**, *A222*, 456.
(32) Bonsall, E. P.; Valentine, L.; Melville, H. W. *Trans. Faraday Soc.* **1952**, *48*, 763.
(33) Burnett, G. M.; Gersmann, H. R. *J. Polym. Sci.* **1958**, *28*, 655.
(34) Suzuki, M.; Miyama, H.; Fujimoto, S. *J. Polym. Sci.* **1958**, *32*, 445.
(35) El-Sabee, M. Z.; Shinouda, H. G.; Morsi, M. A.; Ahmed, A. R.; Mawazini, S. *Makromol. Chem.* **1975**, *176*, 3565.
(36) Szafko, J.; Turska, E. *Makromol. Chem.* **1972**, *156*, 311.
(37) Fukuda, T.; Ma, Y.-D.; Inagaki, H. *Polym. Prepr., Jpn.* **1983**, *32*, 1119.
(38) Bonsall, E. P.; Valentine, L.; Melville, H. W. *J. Polym. Sci.* **1951**, *7*, 39.
(39) Matsuo, K.; Stockmayer, W. H. *Macromolecules* **1977**, *10*, 658.
(40) Benson, S. W.; DeMore, W. B. *Annu. Rev. Phys. Chem.* **1965**, *16*, 397.
(41) Terry, J. O.; Futrell, J. H. *Can. J. Chem.* **1967**, *45*, 2327.
(42) Ma, Y.-D.; Fukuda, T.; Inagaki, H. *Polym. J.* **1983**, *15*, 673.

(43) Matheson, M. S.; Auer, E. E.; Bevilacqua, E. B.; Hart, E. J. J. Am. Chem. Soc. 1949, 71, 497.
(44) Fukuda, T.; Ma, Y.-D.; Nagata, M.; Inagaki, H. Polym. J. 1982, 9, 729.
(45) To avoid confusion, some of the notations given in the original paper[44] have been slightly modified.
(46) North, A. M.; Reed, G. A. Trans. Faraday Soc. 1961, 57, 859.
(47) Ludwico, W. A.; Rosen, S. L. J. Polym. Sci., Polym. Chem. Ed. 1976, 14, 2121.
(48) Flory, P. J. "Principles of Polymer Chemistry"; Cornell University Press: Ithaca, NY, 1953.
(49) Leich, R.; Fuhrmann, J. J. Polym. Sci., Polym. Chem. Ed. 1983, 21, 2215.
(50) Korus, R.; O'Driscoll, K. F. In "Polymer Handbook"; Brandrup, J., Immergut, E. H., Eds.; Academic Press: New York, 1975; Chapter II.
(51) To compute eq 19, we assumed that p_i is given by the terminal-model eq 16. This is not correct in a strict sense, since the failure of the model has been established. However, it should be a valid approximation, since p_i should not be very sensitive to models.
(52) Fukui, K.; Yonezawa, T.; Morokuma, M. J. Polym. Sci. 1961, 49, S11.
(53) North, A. M. In "Reactivity and Structure in Polymer Chemistry"; Jenkins, A. D., Ledwith, A., Eds.; Wiley: London, 1974; Chapter 5.
(54) Horie, K.; Mita, I. Kobunshi 1978, 27, 637.
(55) O'Driscoll, K. F. Pure Appl. Chem. 1981, 53, 617.
(56) Berlin, A. A.; Volfson, S. A.; Enikolopian, N. S. Adv. Polym. Sci. 1981, 38, 89.
(57) Seiner, J. A.; Litt, M. Macromolecules 1971, 4, 308.
(58) Tüdös, F.; Kelen, T.; Berezhnikh, T. F. J. Polym. Sci., Polym. Symp. 1975, 50, 109.
(59) Kamachi, M. Adv. Polym. Sci. 1981, 38, 56.

Free-Radical Copolymerization. 4. Rate Constants of Propagation and Termination for the *p*-Chlorostyrene/Methyl Acrylate System

Yung-Dae Ma, Takeshi Fukuda,* and Hiroshi Inagaki

Institute for Chemical Research, Kyoto University, Uji, Kyoto 611, Japan.
Received April 23, 1984

ABSTRACT: The propagation and termination mechanisms of the free-radical copolymerization of *p*-chlorostyrene and methyl acrylate in the bulk at 40 °C were examined by studying the steady-state as well as non-steady-state polymerizations and thus evaluating the rate constants of propagation and termination individually as a function of feed-monomer composition. The observed rate constant of propagation as well as the copolymer composition studied previously indicated the failure of the terminal model to describe the propagation step of this system. As far as numerical values are concerned, this system is well described by the penultimate model. If one analyzes the data on the steady-state polymerization rate according to the Walling equation, one obtains "apparent" values of the cross-termination factor ϕ ranging from about 70 to as large as 500. The values of the termination rate constant actually observed are well described by the chemically controlled termination model with $\phi = 1$ as well as by the North diffusion model. These results confirm the main conclusions obtained in the previous study on the styrene/methyl methacrylate system.[1]

Introduction

In the preceding paper,[1] the kinetics of free-radical copolymerization of styrene and methyl methacrylate was examined by studying the steady-state as well as non-steady-state polymerizations and thus evaluating the rate constants of propagation and termination individually as a function of monomer composition. This unusual but comprehensive approach has disclosed the striking fact that the so-called terminal model[2,3] is incapable of describing the propagation step of this system, and that the termination step is, as opposed to previous results, well characterized by the Walling factor[4] ϕ close to 1. These results throw a strong doubt on the essential validity of the terminal-model propagation scheme and the prevailing arguments based on it about the mechanism of the termination step. It now seems important to examine a variety of copolymerization systems, especially those exhibiting large values of ϕ according to the conventional analysis, by collecting precise experimental data on the individual rate constants.

In this paper, we examine the bulk copolymerization of *p*-chlorostyrene (pCS, monomer 1) and methyl acrylate (MA, monomer 2) at 40 °C by the same approach as for the above system. The pCS/MA system is interesting because, as has already been reported,[5] its composition curve exhibits small but distinct deviations from the terminal-model curve (the Mayo–Lewis curve[3]). A more definite answer about the model propriety is expected in this study, since the rate equation should generally be more model sensitive than the composition equation is. Another point of interest with this system is that the ϕ value estimated by the conventional method, in which the validity of the terminal model is assumed,[4] is exceptionally large and composition dependent. According to our preliminary results,[6] it is even larger than 500 for a certain range of monomer composition. Whether this is a real phenomenon or not can be ascertained only through the direct evaluation of the termination rate constant.

Experimental Section

Materials. The pCS monomer was synthesized from *p*-dichlorobenzene and purified by a standard process.[5] The commercially obtained MA monomer was purified with special care.[5] 2,2′-Azobis(isobutyronitrile) (AIBN) and 2,2′-azobis(cyclohexane-1-carbonitrile) (ACN) purchased from Nakarai Chemicals Co., Japan, and 4-hydroxy-2,2,6,6-tetramethylpiperidinyl-1-oxy (HTMPO) from Eastman Kodak Co., Rochester, NY, were purified by recrystallization as described previously.[1]

Steady-State Polymerization. The rate of the steady-state polymerization initiated by AIBN was determined by the ampule method. The composition of the copolymer was determined by combustion analysis for carbon and potentiometric titration with silver nitrate for chlorine. The number-average molecular weight M_n and the polydispersity index M_w/M_n were estimated by gel permeation chromatography (GPC) with a column system calibrated with standard polystyrenes. The initiation rate was de-

0024-9297/85/2218-0026$01.50/0